

# Solid State $^{51}\text{V}$ NMR Structural Studies of Vanadium(V) Oxide Catalysts Supported on $\text{TiO}_2$ (Anatase) and $\text{TiO}_2$ (Rutile). The Influence of Surface Impurities on the Vanadium(V) Coordination

HELLMUT ECKERT<sup>1</sup>, GOUTAM DEO<sup>2</sup>, ISRAEL E. WACHS<sup>2</sup> and ANDREW M. HIRT<sup>3</sup>

<sup>1</sup>*Department of Chemistry, University of California, Santa Barbara, Goleta, CA 93106 (U.S.A.)*

<sup>2</sup>*Zettlemoyer Center for Surface Studies and Department of Chemical Engineering, Lehigh University, Bethlehem, PA 18015 (U.S.A.)*

<sup>3</sup>*Materials Research Laboratories, Inc., 720 King Georges Post Road, Fords NJ 08863 (U.S.A.)*

(Received 25 September 1989; accepted 27 September 1989)

## ABSTRACT

Solid state  $^{51}\text{V}$  wideline NMR studies show that under ambient conditions the vanadium(V) oxide surface phases on  $\text{TiO}_2$ (anatase) and  $\text{TiO}_2$ (rutile) supports predominantly possess distorted-octahedral coordination. However, the coordination environment of vanadia is markedly influenced by the presence of impurities in the support materials. Surface contaminants promote the formation of tetrahedral surface vanadia species, which preferentially form at low surface coverages. The presence of these surface impurities depends on the titania preparation method and overshadows the influence, if any, of the bulk  $\text{TiO}_2$  lattice structure (anatase versus rutile). Thus, the strong influence of surface impurities on the  $\text{V}_2\text{O}_5/\text{TiO}_2$  system is most likely responsible for the widely varying claims about differences in the catalytic properties of  $\text{V}_2\text{O}_5/\text{TiO}_2$ (anatase) versus  $\text{V}_2\text{O}_5/\text{TiO}_2$ (rutile) samples.

## INTRODUCTION

$\text{V}_2\text{O}_5$  supported on  $\text{TiO}_2$  is known to be an important oxidation catalyst [1-11], specifically for the partial oxidation of *o*-xylene to phthalic anhydride. Catalytic studies have suggested that  $\text{V}_2\text{O}_5/\text{TiO}_2$ (anatase) is a superior catalyst than  $\text{V}_2\text{O}_5/\text{TiO}_2$ (rutile) for this oxidation [12]. Early studies attributed the higher activity of the  $\text{V}_2\text{O}_5/\text{TiO}_2$ (anatase) to the ease of oxygen evolution under inert environments [2,13]. Vejux and Courtine [13] ascribe the higher activity of the  $\text{V}_2\text{O}_5/\text{TiO}_2$ (anatase) catalyst to the crystallographic fit between pure  $\text{V}_2\text{O}_5$  (010 plane) and pure  $\text{TiO}_2$ (anatase) (010 or 001 plane). Likewise, the lower activity of  $\text{V}_2\text{O}_5/\text{TiO}_2$ (rutile) was attributed to the misfit of the lattice parameters of the two corresponding bulk phases. Since then, these con-

clusions have been strongly disputed with the discovery of a two-dimensional vanadium oxide overlayer phase dispersed on  $\text{TiO}_2$  [1,4,5,8–10]. This overlayer is neither in epitaxial registry with the support, nor does it have a structure corresponding to that of bulk  $\text{V}_2\text{O}_5$  [14].

Wachs et al. employed Raman spectroscopy to examine the nature of the supported vanadium oxide species on  $\text{TiO}_2$  (anatase) and  $\text{TiO}_2$  (rutile) [15]. The surface vanadium oxide Raman bands on  $\text{TiO}_2$  (anatase) were much broader than on  $\text{TiO}_2$  (rutile), corresponding to a wider distribution of surface vanadium oxide species environments. Gasior et al. concluded from comparative studies with  $\text{V}_2\text{O}_5$  supported on  $\text{TiO}_2$  (anatase and rutile) that the surface vanadium species is not stable on  $\text{TiO}_2$  (rutile) and consequently exhibits inferior catalytic properties [16,17]. The lower surface energy of the  $\text{TiO}_2$  (rutile) support was considered to be responsible for this difference [18]. In contrast, Inomata et al. did not find any difference between a series of  $\text{V}_2\text{O}_5/\text{TiO}_2$  (anatase) and  $\text{V}_2\text{O}_5/\text{TiO}_2$  (rutile) catalysts using the  $\text{NO}-\text{NH}_3$  oxidation reaction [19]. Cavani et al. presented data on  $\text{V}_2\text{O}_5/\text{TiO}_2$  (anatase) and  $\text{V}_2\text{O}_5/\text{TiO}_2$  (rutile) for the ammonoxidation of toluene and oxidation of *o*-xylene [20]. Based on their data, they conclude that the structure of  $\text{TiO}_2$ , anatase or rutile, does not change the activity of the catalyst. Van Hengstum et al. studied the effect of  $\text{TiO}_2$  (anatase and rutile) interactions with  $\text{V}_2\text{O}_5$  primarily through the gas phase oxidation of toluene and methanol oxidation [3,21]. These authors conclude that differences between  $\text{V}_2\text{O}_5/\text{TiO}_2$  (anatase) and  $\text{V}_2\text{O}_5/\text{TiO}_2$  (rutile) are largely due to differences in crystal structure rather than surface accumulations of silica and alumina contaminations.

One of the major complications arising from the comparative analysis of the  $\text{V}_2\text{O}_5/\text{TiO}_2$  (anatase) and the  $\text{V}_2\text{O}_5/\text{TiO}_2$  (rutile) catalyst systems is the origin and the nature of the titania supports. The titania supports used in most of these studies were primarily obtained from pigment manufacturers.  $\text{TiO}_2$  supports are usually synthesized from  $\text{TiCl}_4$ , titanium alkoxides, or  $\text{Ti}(\text{SO}_4)_2$  starting materials. Due to intentional introduction, or as a result of manufacturing procedures, a variety of additives/impurities such as K, P, Cl, Al, S, or Si are known to exist on the titania surface [3,6,16]. Thus, in order to gain a fundamental understanding of the  $\text{V}_2\text{O}_5/\text{TiO}_2$  interactions, it is critical that controlled studies be performed with titania surfaces whose surface compositions are well-known.

The present study focuses on the influence of the various titania preparation methods on the resultant  $\text{TiO}_2-\text{V}_2\text{O}_5$  interaction. This issue is addressed by  $^{51}\text{V}$  solid state NMR. Although solid state NMR methods represent a novel and very promising approach to these systems, previous applications to vanadia-based systems have remained scarce [22–28]. In a detailed study, we have recently developed the methodology for the application of  $^{51}\text{V}$  NMR to amorphous vanadium(V) oxide overlayers [29,30]. It has been shown that this characterization technique is capable of sensitively differentiating various va-

nadium bonding configurations present in such overlayers. The distribution of such vanadia environments and its dependence on the preparation methods and the properties of the titania support are the subject of the present research. To this end, the results will be correlated with detailed information about surface impurities as determined by XPS surface analysis.

## EXPERIMENTAL

### Sample preparation

TiO<sub>2</sub>(anatase) samples were prepared by hydrolysis of titanium isopropoxide (calcination temperature 350°C) and by high-temperature flame pyrolysis of TiCl<sub>4</sub> [31,32]. In addition, commercial TiO<sub>2</sub>(anatase) catalysts were obtained from Mobay Corporation (starting material unknown) and Sakai Chemical Industry (starting material: titanium sulfate), and used without any further treatment. TiO<sub>2</sub>(rutile) samples were prepared by hydrolysis [30] or by high-temperature flame pyrolysis of TiCl<sub>4</sub> [31,32], by thermal conversion from commercial TiO<sub>2</sub> (Degussa P-25) at 875°C for 2 h, and by thermal conversion from the TiO<sub>2</sub>(anatase) made from titanium isopropoxide (650°C, 2 h).

TABLE 1

Origin, surface area (*A*) (m<sup>2</sup> g<sup>-1</sup>), wt% V<sub>2</sub>O<sub>5</sub>, surface coverage *θ*, and surface contaminations (in at.%) of the samples under study

Origin	<i>A</i>	Wt%	<i>θ</i>	Surface impurity concentration (at.%)
<i>TiO<sub>2</sub>(anatase)</i>				
Ti-isopropoxide	80	1.0	0.08	Al(0.61), Si(0.73), K(0.08)
Ti-isopropoxide	80	2.5	0.20	not determined
Ti-isopropoxide	80	4.0	0.32	not determined
TiCl <sub>4</sub> pyrolysis	13	1.7	0.77	F(0.41), Si(1.1)
Mobay	10	0.7	0.41	P(3.0), Cl(0.22), K(0.85)
Mobay	10	1.9	1.12	not determined
Sakai-1	97	5.0	0.32	S(1.7), K(0.03), Fe(0.18)
Sakai-2	121	5.0	0.26	F(2.2), S(0.65)
<i>TiO<sub>2</sub>(rutile)</i>				
TiCl <sub>4</sub> hydrolysis	25	1.0	0.27	no impurities detected
TiCl <sub>4</sub> hydrolysis	25	2.5	0.68	not determined
TiCl <sub>4</sub> hydrolysis	25	4.0	1.08	not determined
TiCl <sub>4</sub> pyrolysis	10	1.7	1.00	Si(1.3), S(0.38)
TiO <sub>2</sub> (875°C) <sup>a</sup>	10	1.7	1.00	Si(1.0)
Ti-isopropoxide <sup>b</sup>	13	1.0	0.45	Na(0.17), Si(1.5), Fe(0.56)

<sup>a</sup>Converted from TiO<sub>2</sub> (Degussa P-25) at 875°C for 2 h.

<sup>b</sup>Converted from TiO<sub>2</sub>(anatase) made from Ti-isopropoxide at 650°C for 2 h.

The supported vanadium oxide on  $\text{TiO}_2$  catalysts were prepared by the incipient wetness impregnation method with  $\text{VO}(\text{OC}_2\text{H}_5)_3$  in ethanol or  $\text{VO}(\text{O}-i\text{-C}_3\text{H}_7)_3$  in methanol. The impregnated samples were dried at room temperature for 16 h, dried at 110–120°C for 16 h, and subsequently calcined at 350–450°C to form the supported vanadium oxide on  $\text{TiO}_2$  catalysts. Table 1 summarizes the origins, surface areas (prior to vanadia deposition), vanadia contents, and vanadia surface coverages, determined from Raman spectroscopy. Also included are relative surface concentrations of various impurities, as determined from XPS surface analysis.

### *XPS surface analysis*

Specimens for XPS analysis were prepared by pressing the catalyst powders between stainless steel holders in a polished single crystal silicon wafer. XPS measurements were performed at  $5 \cdot 10^{-9}$  Torr on a Model DS800 XPS surface analysis system, manufactured by KRATOS Analytical Plc, Manchester, United Kingdom. A hemispherical electron energy analyzer was used for electron detection. General survey spectra were collected for each of the catalyst powder specimens. Mg- $\text{K}_\alpha$  X-rays at a power of 360 W were employed in this study. Data were collected in 0.75 eV segments for a total of 1 h using a pass energy of 80 eV for each of the specimens. The electron spectrometer was operated in the fixed analyzer transmission (FAT) mode. Elements detected in each spectrum were identified and concentration estimates were made using typical normalization procedures.

### *Nuclear magnetic resonance studies*

Room-temperature wide-line solid state NMR studies were carried out using a General Electric GN-300 spectrometer, equipped with an Explorer high-speed digitizer and a 7 mm multinuclear MASS-NMR probe (zirconia stator) from DOTY Scientific. Systematic probing of the pulse excitation behavior revealed that the effective 90° pulse length in the catalyst samples is shortened from 7–8  $\mu\text{s}$  in liquid  $\text{VOCl}_3$  to 2.4–3.3  $\mu\text{s}$ , as a result of a strong nuclear electric quadrupole splitting. Spectra were obtained both by the single pulse method and a special quadrupolar echo sequence, previously reported to record undistorted central transitions of half-integer quadrupolar nuclei [33]. The question whether correct relative NMR signal intensities can be obtained from species whose  $^{51}\text{V}$  nutation frequencies differ within the same sample, was addressed by systematic pulse length dependent studies (at a non-selective nutational frequency of 35.7 kHz). A specifically designed model mixture was used, consisting of  $\text{ZnV}_2\text{O}_6$  (distorted octahedral coordination, effective 90° pulse length 2.5  $\mu\text{s}$ ) and  $\text{Tl}_3\text{VO}_4$  (symmetric tetrahedral coordination, effective 90° pulse length 5.8  $\mu\text{s}$ ) in a 1:1 weight ratio.

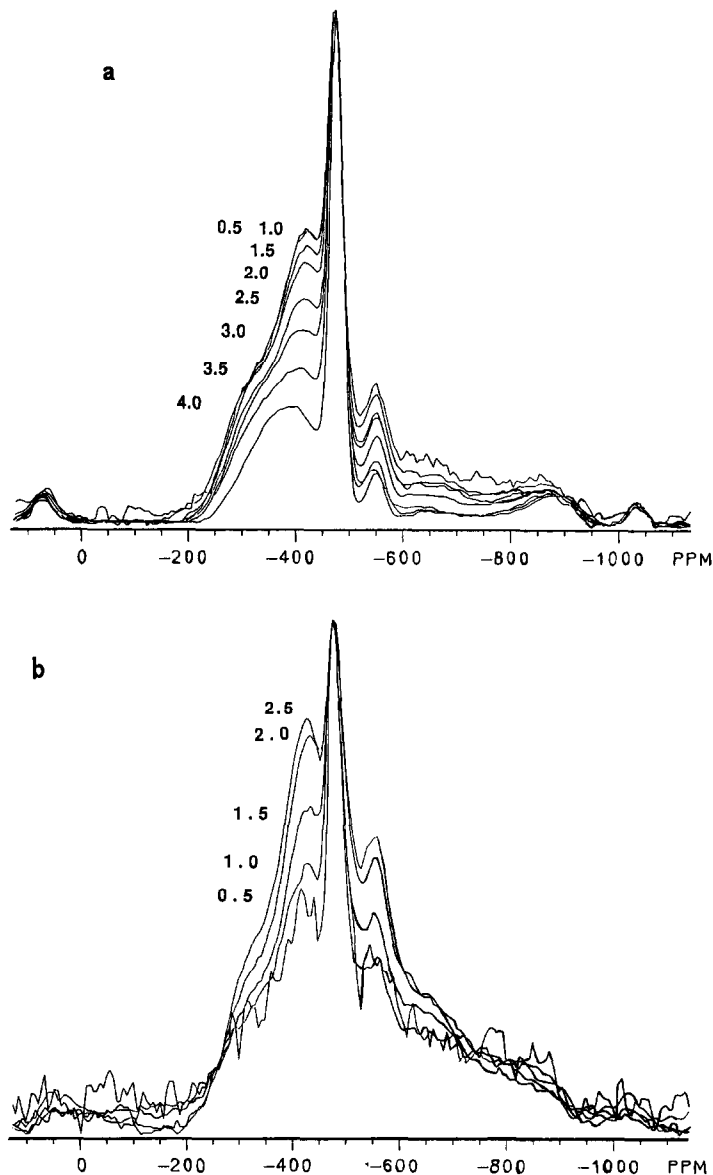


Fig. 1. Pulse length dependence of the  $^{51}\text{V}$  NMR spectrum of a model mixture of  $\text{ZnV}_2\text{O}_6$  and  $\text{Tl}_3\text{VO}_4$  in a 1:1 weight ratio. The respective pulse length used (in  $\mu\text{s}$ ) is indicated at the level of the most downfield relative maximum of the corresponding lineshape. (a) Single-pulse experiment; (b) solid echo sequence  $\theta$ - $\tau$ - $2\theta$  ( $\tau=30 \mu\text{s}$ ). The sharp line at  $-480$  ppm and the sidebands at  $70$  and  $-1030$  ppm belong to  $\text{Tl}_3\text{VO}_4$ ; all other features belong to  $\text{ZnV}_2\text{O}_6$ .

As shown in Fig. 1, the intensity ratios are pulse-length dependent in both methods. While at pulse lengths of 1  $\mu$ s and below essentially identical results are obtained, the single-pulse method underestimates the component with the higher nutational frequency (i.e. with the stronger quadrupolar interaction) at longer pulse lengths. The opposite appears to be true for the echo method. Here, the relative signal area due to this component increases with increasing pulse length, until reaching a maximum at its effective 90° pulse length. At even longer pulse lengths, the contribution of this signal component diminishes again (data not shown). Based on these studies, the single-pulse method with pulse lengths of 1  $\mu$ s or less appears preferable for relative signal quantitation studies of vanadium species with different nutational frequencies. Furthermore, the overall refocusing by the echo method appears to be incomplete, resulting in significantly lower signal-to-noise ratios. Hence the spectra reported below are obtained from simple Bloch decays, using a 1  $\mu$ s pulse length and a 1 s relaxation delay. Chemical shifts are referenced with respect to liquid  $\text{VOCl}_3$ .

## RESULTS AND DISCUSSION

### *XPS surface analysis*

The surface compositions of the different  $\text{V}_2\text{O}_5/\text{TiO}_2$  samples were analyzed by X-ray photoelectron spectroscopy. The detectable atomic surface concentrations of foreign elements (in at.%) are included in Table 1. Detection limits are: 0.01 at.% F, 0.01 at.% Na, 0.20 at.% Al, 0.20 at.% Si, 0.10 at.% P, 0.05 at.% S, 0.05 at.% Cl, 0.02 at.% K, and 0.10 at.% Fe. The XPS technique analyzes the outer 2–5 nm layer and does not provide information about the composition within internal titania pores. Nevertheless, since surface impurities are expected to be distributed over all the surfaces, internal and external, the XPS analysis should be representative of the surface compositions of the various samples. The  $\text{TiO}_2$  samples from Sakai were found to contain large surface concentrations of sulfate. This is expected since these materials are prepared from  $\text{Ti}(\text{SO}_4)_2$ . On the other hand, the  $\text{TiO}_2$  samples prepared from  $\text{TiCl}_4$  were not found to possess any surface chloride, with the exception of commercially obtained Degussa P-25 (as received). Silica was found to be a common surface impurity, with the exception of the samples prepared by low temperature hydrolysis of  $\text{TiCl}_4$ . The high-temperature calcination appears to surface-segregate silica onto the titania surface. The  $\text{TiO}_2$  samples synthesized from titanium isopropoxide contain surface alumina, silica, and traces of potassium oxide in the anatase modification, and surface silica, sodium and iron oxide in the rutile modification. The commercial  $\text{TiO}_2$  (anatase) from Mobay was found to contain significant surface concentrations of phosphorus oxide, potassium oxide, and chloride. Several samples also contain fluoride impurities. Thus, the different titania starting materials and preparation methods result in different concentrations of surface impurities. The XPS surface concentrations

of vanadia agree qualitatively with the vanadia surface concentrations determined independently from Raman spectroscopy as previously discussed.

### *NMR investigations*

Figures 2–5 summarize the spectral data indicating a surprisingly large variability of the NMR lineshapes depending on the source of the  $\text{TiO}_2$  support. In the following, a separate discussion of the various spectral features observed will be given for the anatase and rutile samples, in connection with the preparative details.

#### *Vanadium(V) oxide on $\text{TiO}_2$ (anatase)*

Unfortunately, none of the  $\text{TiO}_2$  (anatase) preparations used resulted in a completely clean surface. In the following, our discussion will therefore center on the comparison of home-made samples (all of which contain substantial surface impurities of silica and other impurities) with commercial materials (whose surfaces are silica-free, but contain various other contaminants such as sulfate, phosphate, and potassium oxide). Figure 2 shows the  $^{51}\text{V}$  NMR spectra of vanadium(V) surface oxide species supported on home-made anatase samples prepared from titanium isopropoxide. The spectra show a near-

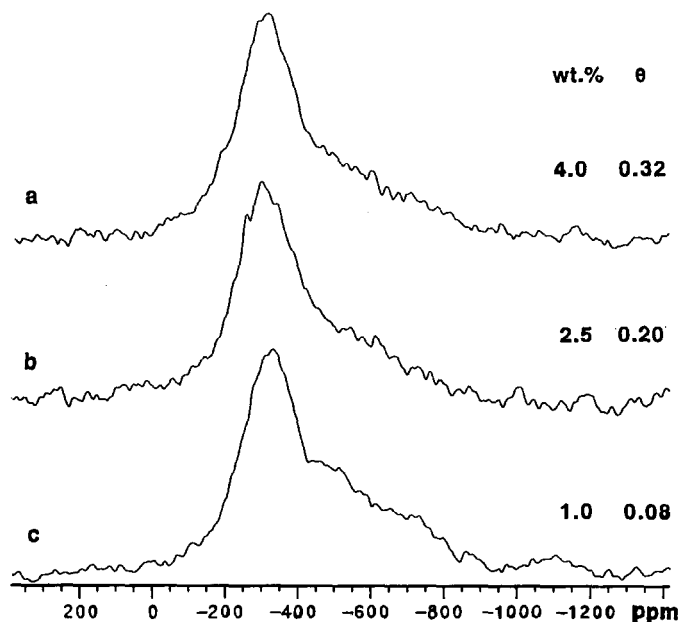


Fig. 2. 79.0 MHz  $^{51}\text{V}$  wideline NMR spectra of surface vanadium(V) oxide on  $\text{TiO}_2$ (anatase) prepared from hydrolysis of titanium isopropoxide. The numerals indicate the overall concentration and the surface coverage of  $\text{V}_2\text{O}_5$ .

to-axial chemical shift powder pattern centered around  $-500$  ppm, the nearly degenerate perpendicular components of the shift tensor being located near  $-300$  ppm, and the parallel component between  $-800$  and  $-900$  ppm. These chemical shifts have to be regarded as average values of a distribution due to the disordered state of vanadium on the surface. Extensive  $^{51}\text{V}$  NMR studies of model compounds have shown that such spectral parameters are unique and characteristic of a vanadium (V) species in a distorted octahedral coordination environment [29,30]. Furthermore, the solid state NMR data confirm that this environment is quite different from that in crystalline  $\text{V}_2\text{O}_5$ , whose chemical shift component along the unique axis is as high as  $-1250$  ppm. Figure 2 thus reveals that the vanadium (V) oxide coordination in these anatase samples is almost exclusively octahedral. In addition, a broad weak resonance contribution to the spectral intensity near  $-500$  to  $-600$  ppm is evident in the isopropoxide-derived sample with the lowest surface coverage, and also in the sample prepared from  $\text{TiCl}_4$  flame pyrolysis (see Fig. 3e). Based on previous model compound studies, this resonance can be attributed to a minor contribution of a tetrahedral, most likely polymeric vanadate chain, species.

Figure 3 shows NMR data obtained on vanadium (V) oxide surface species deposited on various commercial  $\text{TiO}_2$  (anatase) samples. These spectra give clear evidence of a third type of site, whose exact chemical shift tensor components cannot be determined due to extensive peak overlap. However, its powder pattern has a peak maximum at  $-660$  ppm, reminiscent of the tetrahedral surface vanadium (V) oxide species observed in surface-dehydrated anatase and alumina samples [30]. This site appears especially predominant in  $\text{TiO}_2$  (anatase) from Mobay Corporation, whose surface is heavily contaminated with potassium oxide and phosphate impurities. Traces a and b compare two different loadings, suggesting that the tetrahedral site is preferentially occupied at low surface coverage.

Similar impurity effects are also responsible for the very complex  $^{51}\text{V}$  NMR spectrum of surface vanadium (V) oxide on  $\text{TiO}_2$  (anatase) from Sakai Chemical Industry Co. This high-surface area material is prepared from titanium sulfate, and, according to the XPS analysis, has substantial amounts of residual sulfate on the surface. The NMR spectra show that such contaminants play a distinct role in determining the vanadium (V) oxide species distribution at the surface.

In summary, the vanadia coordination on the  $\text{TiO}_2$  (anatase) surface is predominantly distorted-octahedral in all of the samples studied. Commercial anatase catalysts show a substantially larger fraction of the tetrahedral surface vanadia, compared to the home-made materials. Therefore, we conclude that surface impurities such as sulfate and potassium oxide/phosphorus oxide stabilize tetrahedral coordinated vanadia on the surface. We are, however, at present unable to decide, which specific contaminant has the greatest influence. The suspicion that silica might suppress the formation of some four-coordi-



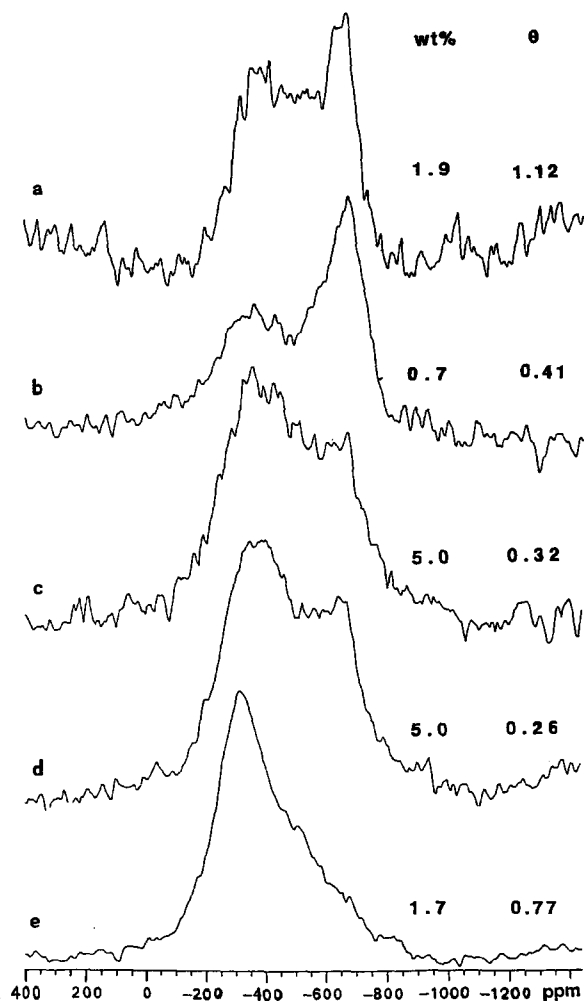


Fig. 3. 79.0 MHz  $^{51}\text{V}$  wideline NMR spectra of surface vanadium(V) oxide on  $\text{TiO}_2$ (anatase) with different sample histories. The numerals indicate the overall concentration and the surface coverage of  $\text{V}_2\text{O}_5$ : (a) commercial  $\text{TiO}_2$ (anatase), Mobay Corporation, 1.9 wt%  $\text{V}_2\text{O}_5$ ; (b) commercial  $\text{TiO}_2$ (anatase), Mobay Corporation, 0.7 wt%  $\text{V}_2\text{O}_5$ ; (c) commercial  $\text{TiO}_2$ (anatase), Sakai, 5 wt%  $\text{V}_2\text{O}_5$ -sample 1 (previously analyzed to contain 2.59 wt% Ba in bulk sample); (d) commercial  $\text{TiO}_2$ (anatase), Sakai, 5 wt%  $\text{V}_2\text{O}_5$ -sample 2 (previously analyzed to contain 0.15 wt% Ba in bulk sample); (e)  $\text{TiO}_2$ (anatase) prepared via pyrolysis of  $\text{TiCl}_4$ .

nated vanadia species has certain merits in view of the results obtained on the  $\text{TiO}_2$ (rutile) samples as discussed below.

#### *Vanadium(V) oxide on $\text{TiO}_2$ (rutile)*

Figure 4 shows  $^{51}\text{V}$  NMR spectra of vanadium(V) oxide supported on the surface of a pure  $\text{TiO}_2$ (rutile) sample prepared by low-temperature  $\text{TiCl}_4$  hy-

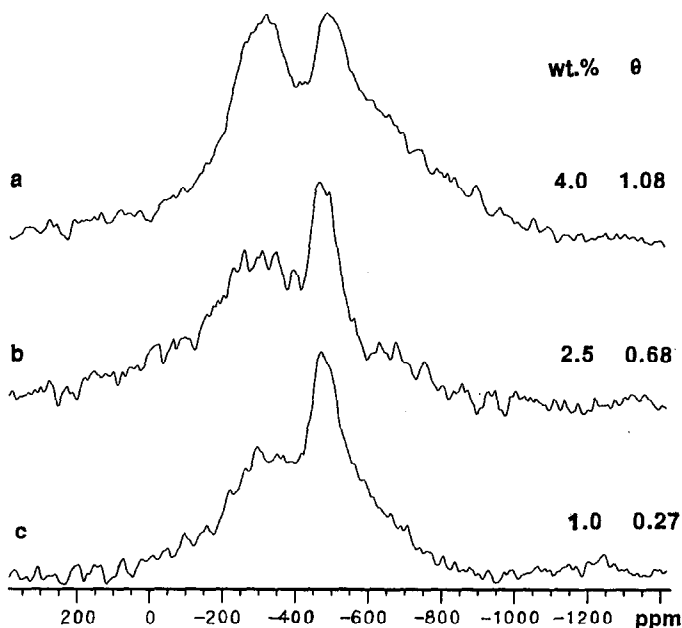


Fig. 4. 79.0 MHz  $^{51}\text{V}$  wideline NMR spectra of surface-vanadium(V) oxide on  $\text{TiO}_2$  (rutile) prepared by hydrolysis of  $\text{TiCl}_4$ . The numerals indicate the overall concentration and the surface coverages of  $\text{V}_2\text{O}_5$ .

drolysis. The spectra show clearly that the octahedral species, already identified in the anatase samples, is the dominant spectroscopic feature here as well. Most significantly, however, substantial signal intensity is observed for a new, sharp signal located near  $-500$  ppm, especially at low surface coverages. The location of this peak and its sharpness suggest a small chemical shift anisotropy, which is consistent with an assignment to a very symmetric, presumably isolated-tetrahedral species. The relative signal area (obtained via peak deconvolution and integration [30]) of the combined tetrahedral species decreases with increasing V(V) concentration from ca. 35% at the lowest surface coverage to ca. 20% at monolayer coverage, hence indicating its preferential formation at low coverages.

Figure 5 shows  $^{51}\text{V}$  NMR spectra of a variety of other home-made rutile samples that were prepared at high temperatures. Sample (a) was prepared by flame pyrolysis of  $\text{TiCl}_4$ , sample (b) was thermally converted from commercial Degussa P-25 titania, and sample (c) was thermally converted from  $\text{TiO}_2$  (anatase), which had been previously prepared via hydrolysis of titanium isopropoxide. The surfaces of all of these samples contain significant amounts of silica contaminants, as revealed by XPS surface analysis, and the NMR spectra show that the octahedral species is the dominant spectroscopic feature here as well. However, the comparison between Figs 4 and 5 clearly illustrates

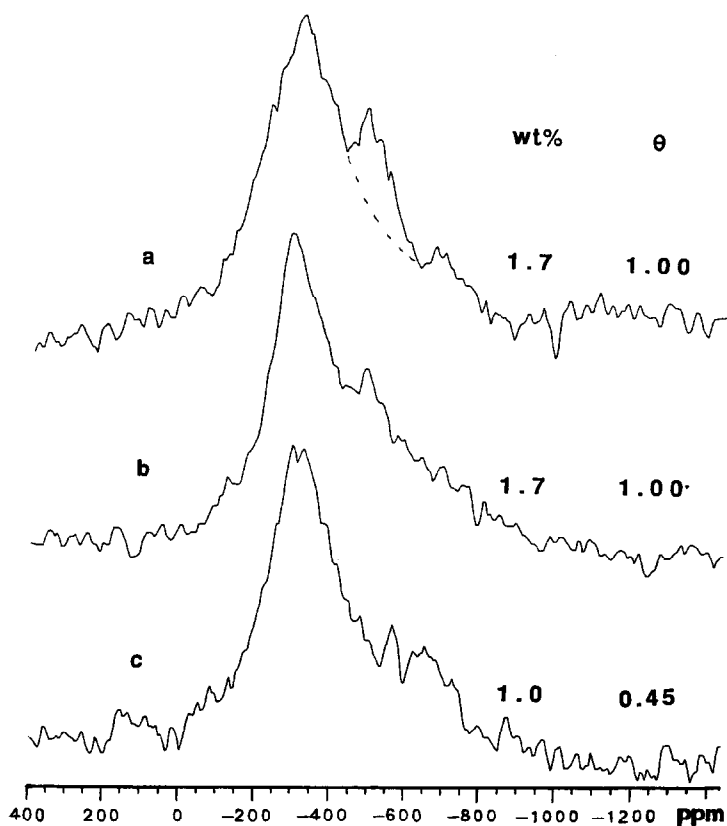


Fig. 5. 79.0 MHz  $^{51}\text{V}$  wideline NMR spectra of surface vanadium(V) oxide on  $\text{TiO}_2$ (rutile) prepared under different conditions. The numerals indicate the overall concentration and the surface coverage of  $\text{V}_2\text{O}_5$ : (a) pyrolysis of  $\text{TiCl}_4$ ; (b) conversion from commercial  $\text{TiO}_2$  (Degussa); (c) conversion from  $\text{TiO}_2$  (anatase), prepared via hydrolysis of titanium isopropoxide.

that the tetrahedral species is much less abundant in samples that have silica surface contaminations and that were prepared at high temperatures. Appreciable amounts of tetrahedral species with a chemical shift near  $-500$  ppm are still retained in the sample prepared from  $\text{TiCl}_4$  flame pyrolysis. Further studies are underway to decide whether these differences arise from surface contamination effects or the differences in preparation temperatures. Low preparation temperatures are expected to increase the concentration of surface defects which might promote formation of this tetrahedral species.

In summary, the coordination of surface vanadia on  $\text{TiO}_2$ (rutile) prepared via different routes is predominantly distorted-octahedral. Preferentially at low surface coverages, the spectra evidence the formation of a highly symmetric tetrahedral species as well. Since we have observed this site thus far only in  $\text{TiO}_2$ (rutile) samples (contaminated or uncontaminated) but never in

TiO<sub>2</sub> (anatase) samples we are tempted to conclude that it may be intrinsically characteristic for rutile surfaces.

## CONCLUSIONS

The results of the present study reveal the suitability of wide-line <sup>51</sup>V NMR in providing the species distribution present in two-dimensional surface vanadium (V) oxide overlayers on metal oxide supports. In the investigation of titania-based systems with low surface areas, the inherently element-selective and quantitative mode of study provides NMR with a distinct advantage over Raman spectroscopy, which is somewhat hampered by the strong background scattering of the support lattice. Under ambient conditions, the coordination of surface vanadium (V) oxide is predominantly distorted-octahedral, both on TiO<sub>2</sub> (rutile) and TiO<sub>2</sub> (anatase), regardless of their sources and preparation conditions. The preliminary results presented here suggest, however, that the bonding state of vanadia on titania-based surfaces also depends on the mode of preparation, and the presence of silica, phosphate, potassium, or sulfate impurities. Specifically, high silica surface contaminations appear to correlate with a predominantly octahedral V(V) environment, whereas sulfate, potassium and/or phosphate impurities can be associated with a tetrahedral vanadium species, whose <sup>51</sup>V NMR peak maximum appears around -660 ppm. The presence of these surface impurities overshadows the influence, if any, of the bulk TiO<sub>2</sub> lattice structure (anatase versus rutile) on the chemical environment of the surface vanadium (V) species. This finding most probably accounts for the widely differing claims about the catalytic properties of V<sub>2</sub>O<sub>5</sub>/TiO<sub>2</sub> (anatase) versus V<sub>2</sub>O<sub>5</sub>/TiO<sub>2</sub> (rutile) catalysts.

Surface contaminants are often added intentionally to improve catalyst performance [34]. The results of this preliminary study suggest that the role of such modifiers lies in changing the nature of the supported vanadium (V) oxide surface species. Our results show that <sup>51</sup>V solid state NMR proves to be a highly sensitive probe for such effects. We note that all of our NMR studies have been conducted on samples under ambient atmospheric conditions, where the surfaces are hydrated. The effect of surface contaminants is most favorably studied under such conditions, since surface dehydration greatly diminishes the fraction of distorted-octahedral vanadia surface species [30], leading to more overlap, and hence lower resolution, in the spectral region of interest. Further detailed studies, addressing the quantitative relationship between the vanadia species distribution, surface coverages and the concentration of the surface contaminants (as determined by XPS) are currently in progress.

## ACKNOWLEDGEMENTS

We would like to thank J.M. Tatibouet of University P. and M. Curie (Paris, France) for providing the titania samples prepared from pyrolysis of TiCl<sub>4</sub>. G. Deo and I.E. Wachs acknowledge support by NSF grant No. CBT-8810741.

## REFERENCES

- 1 F. Roozeboom, M.C. Mittlemeijer-Hazeleger, J.A. Moulin, J. Medema, V.H.J. DeBeer and P.J. Gellings, *J. Phys. Chem.*, 84 (1980) 2783.
- 2 D.J. Cole, C.F. Cullis and D.J. Hucknall, *J. Chem. Soc.*, 72 (1976) 2185.
- 3 A.V. Van Hengstum, J.G. Van Ommen, H. Bosch and P.J. Gellings, *Appl. Catal.*, 8 (1983) 369.
- 4 G.C. Bond and P. Konig, *J. Catal.*, 77 (1982) 309; G.C. Bond and K. Brukman, *Faraday Discuss. Chem. Soc.*, 72 (1981) 235.
- 5 I.E. Wachs, S.S. Chan and R.Y. Saleh, *J. Catal.*, 91 (1985) 366.
- 6 I.E. Wachs, R.Y. Saleh, S.S. Chan and C.C. Chersich, *Appl. Catal.*, 15 (1985) 339.
- 7 R.Y. Saleh, I.E. Wachs, S.S. Chan and C.C. Chersich, *J. Catal.*, 98 (1986) 102.
- 8 I.E. Wachs, F.D. Hardcastle and S.S. Chan, *Mater. Res. Soc. Symp. Proc.*, 111 (1988) 353.
- 9 F.D. Hardcastle and I.E. Wachs, *Proc. 9th Int. Congr. Catal.*, 3 (1988) 1449.
- 10 I.E. Wachs, J.M. Jehng and F.D. Hardcastle, *Solid State Ionics* 32/33 (1988) 904..
- 11 P.J. Gellings, in G.C. Bond and G. Webbs (Eds), *Specialist Periodical Report on Catalysis*, Vol. 7, The Royal Society of Chemistry, London 1985, pp. 105-124.
- 12 M.S. Wainwright and N.R. Forster, *Catal. Rev.*, 19 (1979) 211.
- 13 A. Vejux and P. Courtine, *J. Solid State Chem.*, 23 (1978) 93.
- 14 R. Kozlowski, R.F. Pettifer and J.M. Thomas, *J. Phys. Chem.*, 87 (1983) 5176.
- 15 I.E. Wachs, R.Y. Saleh and S.S. Chan, *Am. Chem. Soc. Div. Petrol. Chem.*, 31 (1986) 272.
- 16 M. Gasior, I. Gasior and B. Grzybowska, *Appl. Catal.*, 10 (1984) 87.
- 17 M. Gasior, J. Haber and T. Machej, *Appl. Catal.*, 33 (1987) 1.
- 18 J. Haber, T. Machej and T. Czeppe, *Surf. Sci.*, 151 (1985) 301.
- 19 M. Inomata, K. Mori, A. Miyamoto, T. Ui and Y. Murakami, *J. Phys. Chem.*, 87 (1983) 754.
- 20 F. Cavani, G. Centi, E. Foresti, F. Trifiro and G. Busca, *J. Chem. Soc. Faraday Trans. 1*, 84 (1988) 237.
- 21 A.J. Van Hengstum, J.G. Van Ommen, H. Bosch and P.J. Gellings, *Proc. Int. Congr. Catal.*, 4 (1984) 297.
- 22 V.M. Mastikhin, O.B. Lapina and L.G. Simonova, *React. Kinet. Catal. Lett.*, 24 (1984) 127.
- 23 V.M. Mastikhin, O.B. Lapina, V.N. Krasilnikov and A.A. Ivakin, *React. Kinet. Catal. Lett.*, 24 (1984) 119.
- 24 T.P. Gorshkova, R.I. Maksimovskaya, D.V. Tarasova, N.N. Chumachenko and T.A. Nikoro, *React. Kinet. Catal. Lett.*, 24 (1984) 107.
- 25 L.R. Le Costumer, B. Taouk, M. Le Meur, E. Payen, M. Guelton and J. Grimblot, *J. Phys. Chem.*, 92 (1988) 1230.
- 26 B. Taouk, H. Guelton, J. Grimblot and J.P. Bonnelle, *J. Phys. Chem.*, 92 (1988) 6700.
- 27 K.V.R. Chary, V.V. Rao and V.M. Mastikhin, *J. Chem. Soc. Chem. Commun.*, (1989) 202.
- 28 K.I. Zamarev and V.M. Mastikhin, *Colloids Surfaces*, 12 (1984) 401.
- 29 H. Eckert and I.E. Wachs, *Mater. Res. Soc. Symp. Proc.* 111 (1988) 455.
- 30 H. Eckert and I.E. Wachs, *J. Phys. Chem.*, 93 (1989) 6796.
- 31 J.M. Tatibouet, *Bull. Soc. Chim. Fr.*, (1986) 18.
- 32 M. Formenti, S. Julliet, T. Meriaudeau, S.G. Tichner and P. Vergnon, *J. Colloid Interface Sci.*, 39 (1972) 79.
- 33 A.C. Kunwar, G.L. Turner and E. Oldfield, *J. Magn. Reson.*, 69 (1986) 124.
- 34 A.V. Van Hengstum, J. Pranger, J.F. Van Ommen and P.J. Gellings, *Appl. Catal.*, 11 (1984) 317.